JOURNAL OF THE MECHANICAL BEHAVIOR OF BIOMEDICAL MATERIALS 28 (2013) 462–470

Available online at www.sciencedirect.com

ScienceDirect

www.elsevier.com/locate/jmbbm

Research paper

Large amplitude oscillatory shear properties of human skin

E. Lamers[a,*], T.H.S. van Kempen[b], F.P.T. Baaijens[a], G.W.M. Peters[c], C.W.J. Oomens[a]

[a]Soft Biomechanics & Tissue Engineering, Biomedical Engineering, Eindhoven University of Technology, Den Dolech 2, Gem-Z. 4.103, PO Box 513, 5600 MB Eindhoven, The Netherlands

[b]Cardiovascular Biomechanics, Biomedical Engineering, Eindhoven University of Technology, PO Box 513, 5600 MB Eindhoven, The Netherlands

[c]Materials Technology Institute, Mechanical Engineering, Eindhoven University of Technology, PO Box 513, 5600 MB Eindhoven, The Netherlands

ARTICLE INFO

Article history:
Received 26 October 2012
Received in revised form
23 January 2013
Accepted 30 January 2013
Available online 9 February 2013

Keywords:
Human skin
Large amplitude oscillatory shear (or LAOS)
Rheology
Digital Image Correlation (or DIC)

ABSTRACT

Skin is a complex multi-layered tissue, with highly non-linear viscoelastic and anisotropic properties. Thus far, a few studies have been performed to directly measure the mechanical properties of three distinguished individual skin layers; epidermis, dermis and hypodermis. These studies however, suffer from several disadvantages such as skin damage due to separation, and disruption of the complex multi-layered composition. In addition, most studies are limited to linear shear measurements, i.e. measurements with small linear deformations (also called small amplitude oscillatory shear experiments), whereas in daily life skin can experience high strains, due to for example shaving or walking. To get around these disadvantages and to measure the non-linear mechanical (shear) behavior, we used through-plane human skin to measure large amplitude oscillatory shear (LAOS) deformation up to a strain amplitude of 0.1. LAOS deformation was combined with real-time image recording and subsequent digital image correlation and strain field analysis to determine skin layer deformations. Results demonstrated that deformation at large strains became highly non-linear by showing intra-cycle strain stiffening and inter-cycle shear thinning. Digital image correlation revealed that dynamic shear moduli gradually decreased from 8 kPa at the superficial epidermal layer down to a stiffness of 2 kPa in the dermis. From the results we can conclude that, from a mechanical point of view, skin should be considered as a complex composite with gradually varying shear properties rather than a three layered tissue.

1. Introduction

Skin is a complex tissue, which is generally divided in three layers: the epidermis, the dermis and the hypodermis. Based on its composition, the epidermis can be further divided into the stratum corneum, which is a layer that mainly comprises dead corneocytes and the viable epidermis consisting of living cells. The primary components of the

*Correspondence to: Biomedical Engineering, Eindhoven University of Technology, PO Box 513, 5600 MB Eindhoven, The Netherlands. Tel.: +31 402473027; fax: +31 402447355.
E-mail address: E.Lamers@tue.nl (E. Lamers).

1751-6161/$ - see front matter © 2013 Elsevier Ltd. All rights reserved.
http://dx.doi.org/10.1016/j.jmbbm.2013.01.024

dermis are collagen and elastin, embedded in a ground substance and water. The hypodermis is the adipose layer containing mainly adipocytes embedded in connective tissue. Currently much effort is put in advancing the knowledge on the mechanical behavior of each of these skin layers for several reasons, such as razor blade design for shaving, cosmetics, and tissue engineering applications (Bhushan and Tang, 2011; Cowley and Vanoosthuyze, 2012; Derler and Gerhardt, 2012; MacNeil, 2008).

The mechanical properties of skin have been extensively analyzed both in vitro and in vivo and results revealed that skin mechanical properties are dependent on several factors, such as ageing, anatomical region, orientation, and hydration (Annaidh et al., 2012; Boyer et al., 2012; Gerhardt et al., 2009; Girardeau et al., 2009; Hendriks et al., 2004; Krueger et al., 2011; Liang and Boppart, 2010; Minematsu et al., 2011; Tang et al., 2010; Zahouani et al., 2011). Generally these studies consider skin to be a homogeneous tissue. However, for a more detailed mechanical analysis skin should be analyzed as a non-linear viscoelastic, anisotropic, and multilayered composite (Meyers et al., 2008; Oomens et al., 1987). With these considerations in mind, several studies were performed to find the mechanical properties of individual skin layers (Geerligs et al., 2011b; Geerligs et al., 2011a; Holt et al., 2008). Geerligs et al. (2011a) and Holt et al. (2008) analyzed deformation of individual skin layers by small amplitude oscillatory shear (SAOS) measurements. The studies respectively demonstrated that viscoelasticity of the individual skin layers was linear up to a shear strain amplitude (γ_0) of 0.005 and a frequency up to at least 10 rad/s. In addition, Geerligs et al. (2011b) performed an indentation study on the epidermis, and found reduced Young's moduli being approximately 100 times larger than shear moduli.

Although measurements on individual skin layers seem attractive to directly assess the mechanical properties, there are several disadvantages. Skin layers are either mechanically or chemically separated, resulting in structural disruption and leading to altered mechanical behavior. Another potential disadvantage encountered by measuring individual skin layers is that excised individual layers may become too thin for accurate measurements (i.e. stratum corneum), introducing an additional error. One possible way to overcome this problem is stacking of multiple layers (Geerligs et al., 2011a). Still, frictional artifacts of the layers may affect the measurements. To overcome problems encountered with mechanical testing of separate layers, Gerhardt et al. (2012) recently developed a method to assess through-plane skin deformation by combining oscillatory shear experiments and real-time recording with digital image correlation (DIC) and strain field analysis, to determine the local displacement of each individual layer and demonstrated this method on porcine skin.

From a mechanical point of view, the concept that skin is a three layered tissue is too simple. It is a complex tissue in which biologically distinctive layers can be observed but where the mechanical properties vary gradually. Therefore, the aim of our study was to measure the shear properties of through-plane human skin *in vitro*. In the current study large amplitude oscillatory shear (LAOS) deformation of through-plane fresh human skin was measured and recorded *in vitro*.

To measure the actual shear deformation within the skin layers, DIC was performed on through-plane skin as described by Gerhardt et al. (2012). Prior to the tests, the lateral sides of the skin received a speckle pattern by paint brushing and subsequently shear deformation was real-time video recorded with a stereo-microscope equipped with a camera (Pan et al., 2009). In addition, the applied oscillatory strain and torsion were recorded. Subsequently, an analysis of the LAOS was performed (Hyun et al., 2011). LAOS shows the transition of materials from a linear to non-linear shear behavior by increasing the strain amplitude at a constant frequency (Ewoldt et al., 2008; Hyun et al., 2011; Wilhelm, 2002).

2. Materials and methods

2.1. Sample preparation

Human skin was obtained from female patients with an age ranging from 34 to 54 years old, undergoing abdominal plastic surgery. The patients gave informed consent for the use of their skin for research purposes, under a protocol approved by the ethics committee of the Catharina Hospital, Eindhoven, The Netherlands.

Within 2 h after excision by the surgeon, skin was transferred to the laboratory and processed. The skin was stretched with forceps on a stainless steel plate (Geerligs et al., 2011b). Subsequently, skin slices of 1.0 ± 0.2 mm thickness (comprising the stratum corneum (SC), epidermis and dermis) were obtained with an electric dermatome (D42, Humeca, The Netherlands). The slices were then punched into $8 \times 8\ mm^2$ pieces and placed in Hank's Balanced Salt Solution (HBSS, Lonza Biowhittaker, Switzerland) supplemented with 5% penicillin/streptavidin and 0.5 mg/ml Fungin. Samples were stored maximally 2 days at 4 °C.

One lateral edge of each skin sample was airbrushed with black paint (custom micron, Iawata, Lion Art, The Netherlands) prior to mechanical testing of the skin. The paint was then allowed to dry for one minute and subsequently the sample was placed back in a small volume of HBSS until use.

2.2. Experimental setup

All shear measurements were performed on a strain-controlled rheometer (ARES LS-LC, Rheometric Scientific, USA) equipped with a Peltier environmental control unit set to a temperature of 37 °C. A stereo-microscope (SZ11, Olympus, Germany) with a monochromatic ccd-camera (Imagingscience, Germany) was placed next to the rheometer to visualize shear deformation of skin. A high precision linear stage was placed on the motor of the rheometer to enable precise positioning of the samples relative to the plane end face of the rheometer tool (Gerhardt et al. 2012).

A mechanical setup was used as described by Gerhardt et al. (2012) (see Fig. 1). Briefly, a sample was adhered eccentrically to one edge of a $50 \times 8 \times 5\ mm^3$ steel, custom made bar with glue (power gel, Pattex®) to prevent slipping (Nicolle and Palierne, 2012). The bar was then attached to the rheometer and approached to the bottom plate. Upon approach the sample was pressed on the glue containing

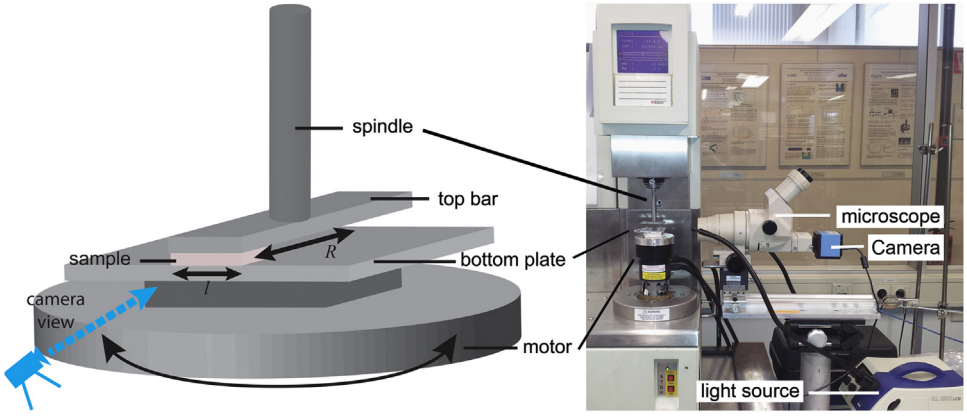

Fig. 1 – (a) Schematic representation of the placement of skin between a top bar and bottom plate. *l* represents the length of the sample and *R* the radius of the top bar. (b) Experimental setup to visualize and measure oscillatory skin deformation.

bottom plate with a normal force between 10 and 30 mN, and the sample was allowed to adhere for 1 min. For precise measurements, adhesion of the sample to the bottom plate was monitored by microscope visualization. The orientation of the Langer lines was at random. Measurements were performed by imposing an oscillatory shear deformation with strain amplitudes (γ_o) ranging from 0.01 to 0.1 and frequencies (f) ranging from 0.2 to 5 Hz. Measurements at a given strain amplitude and frequency were performed for 100 s. Within 1 min after the measurement had finished, a new measurement was started. Finally, the first measurement was repeated after having finished all other measurements.

The response of the tissue was recorded with the torque transducer of the rheometer. To enable analysis of the LAOS deformation, analog voltage outputs of the rheometer were used as described in detail (Hyun et al., 2011; Wilhelm, 2002). In short, the output of the rheometer was connected to an analog-to-digital converter card such that raw strain and torque signals could be stored on a stand-alone pc.

A sinusoidal strain $\gamma(t)$:

$$\gamma(t) = \gamma_0 \sin \omega t \tag{1}$$

was applied to the sample with ω the angular frequency and γ_0 the strain amplitude. As the sample was placed eccentrically, at the edge of the bar with a radius R of 25 mm, the actual shear stress τ was calculated from the measured torque M

$$\tau = \frac{M}{l^2(R - l/2)} \tag{2}$$

where l is the length (8 mm) of the sample. The non-linear shear stress response upon a sinusoidal deformation can in general be written as a Fourier series (Ewoldt et al., 2008; Hyun et al., 2011; Wilhelm, 2002)

$$\tau = \gamma_0 \sum_{n=\text{odd}} G'_n \sin(n\omega t) + G''_n \cos(n\omega t) \tag{3}$$

with G'_n and G''_n the Fourier coefficients that can be related to viscoelastic moduli. Because of odd symmetry between the strain and stress signal, only odd harmonics are expected in the stress response. In the linear viscoelastic regime, all moduli in Eq. (3) vanish except G'_1 and G''_1 which are known as the storage and loss modulus, respectively.

2.3. *Analysis of large amplitude oscillatory strain (LAOS)*

To analyze the LAOS data the raw strain and torque signals where filtered using MATLAB 2010a (Mathworks, Natick, MA, USA) and the Fourier coefficients as defined in Eq. (3) with $n=11$ harmonics were calculated. Higher harmonics were attributed to noise. The viscoelastic behavior of the skin was subsequently visualized using Lissajous plots. An elastic Lissajous plot was obtained by plotting the stress versus the strain, whereas in a viscous Lissajous plot the stress was plotted against strain-rate. Deformations within the linear viscoelastic regime gave elliptic Lissajous curves, and a deviation from this elliptic shape indicated non-linear behavior. To quantify the non-linear viscoelastic response, two moduli as introduced by Ewoldt et al. (2008) were used (see also Fig. 2). The minimum-strain modulus (G_M) is tangent modulus at zero strain. The large-strain modulus (G_L) is the secant modulus at maximum strain. G_M and G_L were calculated according to

$$G_M \equiv \left.\frac{d\sigma}{d\gamma}\right|_{\gamma=0} = \sum_{n=\text{odd}} nG'_n \tag{4}$$

$$G_L \equiv \left.\frac{d\sigma}{d\gamma}\right|_{\gamma=\gamma_0} = \sum_{n=\text{odd}} nG'_n(-1)^{n-1/2} \tag{5}$$

A strain stiffening ratio, S, was subsequently defined as

$$S = \frac{G_L - G_M}{G_L} \tag{6}$$

Strain stiffening ratio $S=0$ indicated a linear response, $S>0$ indicated intra-cycle strain stiffening and $S<0$ indicated strain softening.

2.4. *Digital image correlation*

The deformation of the skin was recorded using a monochromatic ccd-camera. The 8 bit-gray value (640 × 480 pixels) movies were acquired at a frame rate of 30 frames/s and further processed for DIC. At each magnification used (× 40–80), the pixel resolution was determined with a microscope calibration reticule. The resolution of the images was

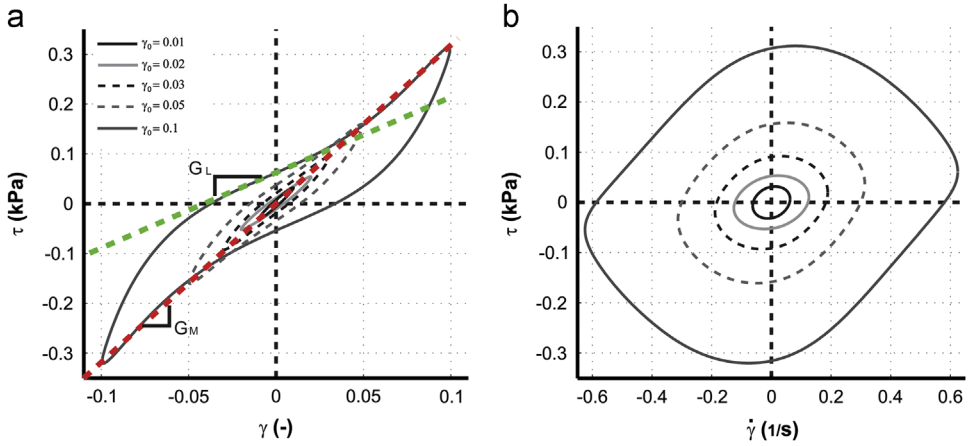

Fig. 2 – (a) Elastic and (b) viscous Lissajous curves at applied γ_0=0.01, 0.02, 0.03, 0.05 and 0.1 with a frequency of 1 Hz, from >10 samples per patient n=5 patients. G_L denotes the secant (large) modulus at maximum imposed strain. G_M denotes the tangent (minimum-strain) modulus at γ=0.

1.9–4.0 μm/pixel, producing a total field of view between 1.2–2.6 mm in width and 0.9–1.9 mm in height.

After acquisition, the shear deformation movies were split into separate images with FIJI software (ImageJ, La Jolla, USA), and analyzed by DIC software (Aramis v5.4.1-5, Gom optical measuring techniques, Braunschweig, Germany).

In the field of view a grid is defined ($x \times y$ grid points) with a spacing of 15 and 21 pixels (spatial grid resolution between 28 and 84 μm). Around every grid point a rectangular area, called a facet, is defined with sizes between 41 and 51 pixels (78–200 μm). Spacing and facet size both depend on magnification and sample thickness. These facets were used for determining the displacements of the grid points. For that, every facet from the initial image of the undeformed state is shifted horizontally and vertically and compared with the next image until a part in the second image is found that correlates best with the initial facet. The position of the shifted facet is the new position of the original grid point and the grid point displacement can be calculated. The distances between a grid point and its directly surrounding grid point in the reference and in the deformed state are used to calculate the local strains (see next paragraph).

The software directly calculated the shear strain. The background of this calculation is shortly explained in the next section.

2.5. Strain analysis

For each grid point the local deformation gradient matrix $\mathbf{F}(x_0)$ defined by

$$\mathbf{F}(x_0) = (\nabla_0\, x)^T \tag{7}$$

is estimated from the relative displacements of the surrounding grid points. Since 2D displacements are measured in the skin cross section, a 2D estimate $\widehat{\mathbf{F}}$ (the "hat" indicates estimates and not the exact values) for $\mathbf{F}$ is obtained, i.e.

$$\widehat{\mathbf{F}} = \begin{bmatrix} \widehat{F}_{11} & \widehat{F}_{12} \\ \widehat{F}_{21} & \widehat{F}_{22} \end{bmatrix} \tag{8}$$

The procedure for determining the estimate values of $\widehat{F}_{ij}$, $\{i,j=1,2\}$ was implemented in the original digital image correlation code, as originally described by Geers et al.(1996). In case of a simple shear deformation the deformation gradient matrix $\mathbf{F}$ is given by

$$\mathbf{F} = \begin{bmatrix} 1 & \gamma \\ 0 & 1 \end{bmatrix} \tag{9}$$

where $\gamma(x_0)$ is the position dependent shear strain. In the following we will present results only for the component $\mathbf{F}(x_0)_{12}=\gamma(x_0)$. Moreover, the results for grid points at the same heights, i.e. all $\gamma(x_0,y_0=\text{constant})$ will be averaged leading to a shear strain $\gamma(y_0)$ only.

2.6. Statistics

Data obtained from the experiments were statistically analyzed with IBM SPSS for Windows (SPSS 19.0) An analysis of variance with the *post-hoc* Tukey test was performed to determine the influence of inter- and intra-patient differences on shear stress. Probability levels of $p<0.05$ were considered significant.

3. Results

3.1. Sample preparation for rheometer and DIC measurements

Upon excision with the dermatome, the dermis was clearly recognizable as a clear white layer and sample thickness was consistently between 0.8 and 1.2 mm. Prior to airbrushing the skin samples were removed from the HBSS, which resulted in immediate contraction, complicating airbrushing at the lateral sides of the samples. The complications with airbrushing were overcome by using forceps to expose the lateral side and placing it in such a manner that the side was completely exposed.

Possible heterogeneous contraction of the sample after placement under the rheometer was as good as possible

circumvented by homogeneously gluing the skin sample to both plates and the application of a small normal force.

3.2. *Variations within and between patients*

A graph of the maximum shear stress separated per patient indicated that (1) intra-patient variation increased with increasing strain amplitude and (2) the magnitude of intra-patient variations in shear stress (Fig. 3).

3.3. *Overall skin behavior*

Elastic and viscous Lissajous curves of the measured stress versus the applied strain and strain rate, respectively (Fig. 2) at a frequency of 1 Hz both demonstrated that overall skin response is altered upon an increasing strain from linear deformation at a strain amplitude γ_0=0.01, to a non-linear deformation at γ_0=0.1. At these high strain amplitudes, the Lissajous curves displayed two phenomena as defined in literature elsewhere (Ewoldt et al., 2008): (1) Intra-cycle strain stiffening, which was observed as a deviation from concave to convex in the high strain region of the the elastic Lissajous curves (from γ_0=0.03, Fig. 2a). (2) Intra-cycle shear thinning, which was observed as a deviation from an elliptical to non-elliptical curve in the viscous Lissajous curves (from γ_0=0.03; Fig. 2b). A more detailed description of these phenomena can be found in Ewoldt et al. (2008). Despite these nonlinear effects, G_L for the overall behavior was surprisingly equal for all applied strain amplitudes at f=1 Hz with an average value of 3.03±0.21 kPa (data not shown). However, this is not a general trend; for f=0.2 Hz, G_L increased from 2.2 kPa to 2.75 kPa with strain amplitude, whereas at f=5 Hz, G_L decreased from 4.28 kPa to 3.53 kPa with an increasing strain amplitude.

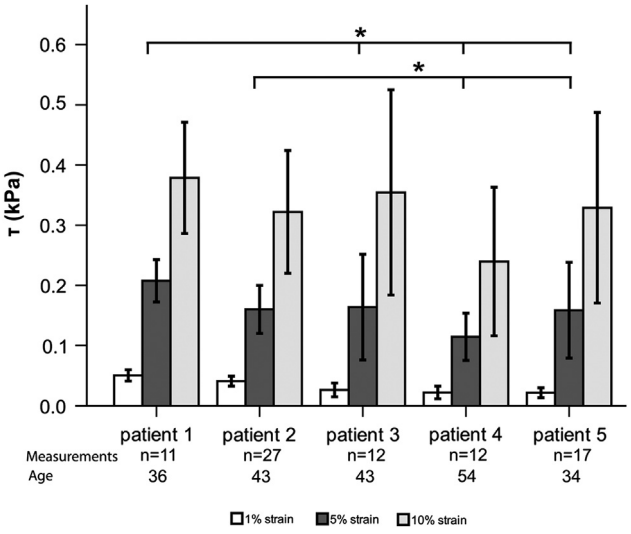

Fig. 3 – Plot of intra- and inter-patient variations in shear stress. Error bars represent the 95% confidence limits. * represents significant difference (p<0.05).

At all strain amplitudes and frequencies, the elastic component of the skin behavior dominated the viscous component indicated by the small area enclosed by the elastic Lissajous curves.

Startup oscillation Lissajous curves (i.e. showing the Lissajous plot from the start of an experiment) were created to show how and how fast the stress response reached a steady state. About 1 s was required for the rheometer to reach a steady oscillatory shear at the imposed strain amplitude (1/3 cycles at a frequency of 0.2 Hz, 1 cycle at 1 Hz, and 5 cycles at 5 Hz; see Fig. 4). Comparing the startup Lissajous plots at all frequencies showed that skin quickly adapted towards the applied strain amplitudes and reaches a steady cyclic stress response in about 2 s (black line in Fig. 4).

To determine how the overall intra-cycle strain stiffening was related to the frequency, we compared frequencies of 0.2 Hz, 1 Hz, and 5 Hz at strain amplitudes of 0.01, 0.05, and 0.1, by determining the strain stiffening ratio S from the Lissajous curves (Fig. 5). At γ_0=0.01, strain stiffening appeared to be absent at all frequencies ($S \approx 0$). At higher strain amplitudes however, strain stiffening became clearly visible at all imposed frequencies ($S > 0$). It was further demonstrated that strain stiffening was not affected by frequency in the used range; at γ_0=10% for example, S=0.44–0.46 at the three tested frequencies.

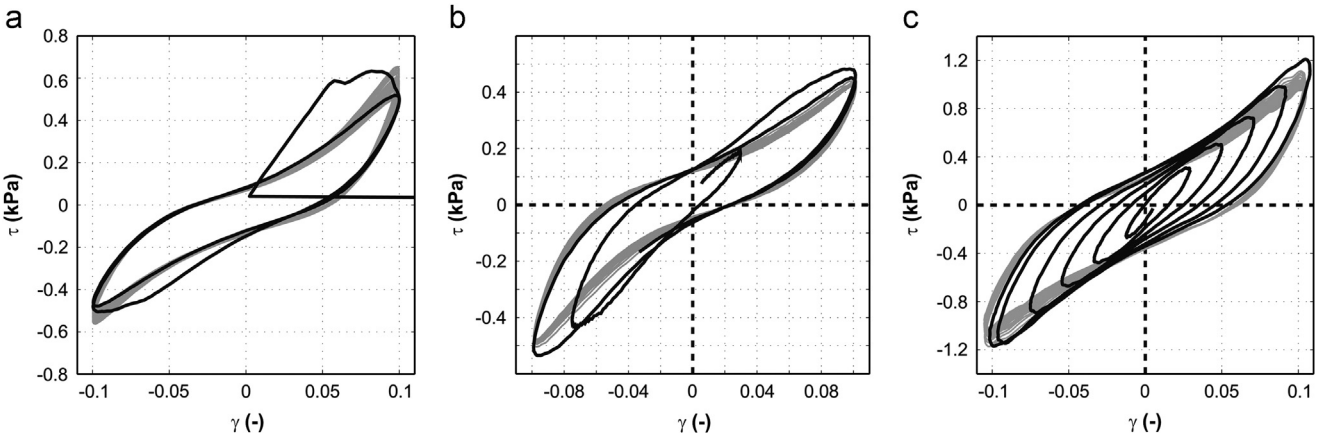

Fig. 4 – Startup–Lissajous curve of skin deformation at γ_0=0.1 and a frequency of (a) 0.2 Hz, (b) 1 Hz, and (c) 5 Hz. The black line indicates the adaptation of skin to the strain amplitude. Gray line indicates oscillations after adaptation. Note that 1 s is required for the rheometer to reach steady state in γ(t).

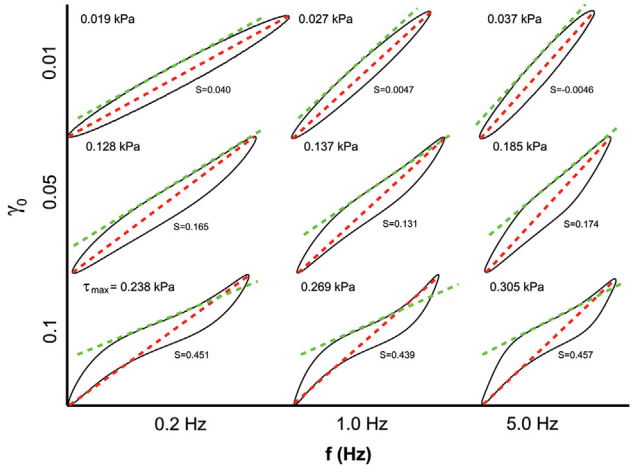

Fig. 5 – Elastic Lissajous curves (τ vs. γ) generated from oscillatory tests with various strain amplitudes and frequencies. The maximum shear stress τ_{max} is indicated above each curve. The red dotted line indicates the secant modulus G_L. The green dotted line indicates the tangent modulus G_M. The strain stiffening ratio S between the G_L and G_M is given underneath each curve (For interpretation of the references to color in this figure legend, the reader is referred to the web version of this article.).

It is important to notice that results presented so far are related to overall skin behavior. In the next section, we will represent similar results but then related to different layers, i.e. as a function of position in the skin thickness direction.

3.4. *Digital image correlation*

Digital image correlation (DIC) was performed on images with γ_0=0.01–0.1 (movies 1–3). For the large strains as well as high frequencies correlation was difficult and often failed. From the images it was observed that skin deformation was heterogeneous over the thickness and sometimes large variations in the shear directions were observed. By averaging results in grid points at the same heights most of these variations were smoothed.

Supplementary material related to this article can be found online at http://dx.doi.org/10.1016/j.jmbbm.2013.01.024.

3.5. *Decomposition of human skin into separate skin layers*

Lissajous plots were created for different layers from recorded oscillatory stress data versus time lapsed local skin deformation ($\gamma(\gamma,t)$) from DIC (Fig. 6; n=25, 5 skin samples per patient). The dermis was at all strain amplitudes significantly more deformed than the epidermis ($p<0.01$). In addition, time revolved deformation at γ_0=0.1 was non-linear in all layers, as strain-stiffening is clearly observed at all layers. At γ_0=0.05 only the dermis showed non-linear behavior, whereas deformation in both the epidermis and papillary region were linear.

3.6. *Secant modulus*

A clear general trend was observed in the DIC-results; hence the secant shear modulus for f=1 Hz at maximal deformation (G_L) was averaged per height layer of ≥6 samples per patient, in 5 patients (see Fig. 7). DIC results of skin layer deformation at γ_0=0.01–0.1 confirmed that, for f=1 Hz, the secant shear modulus was independent of the applied strain amplitude. Moreover, it was clearly shown that the highest shear modulus was found in the top layer of the epidermis, with ~8 kPa maximum. When descending into skin, the stiffness gradually decreased to ~2 kPa for the lower layers of the reticular dermis. At γ_0=0.1 however, the dispersion in results was much larger than for the other strains, which is reflected in the increasing 95% confidence limits. This was mainly due to correlation problems with DIC.

4. Discussion

The aim of the current study was to measure the large amplitude oscillatory shear properties of individual skin layers within through-plane skin samples (i.e. epidermis and dermis) *in vitro*. The results demonstrated that skin response upon increasing strain amplitudes was viscoelastic and non-linear. With increasing strain amplitudes, skin displayed both intra-cycle strain stiffening and inter-cycle shear thinning. Decomposition of the strain into deformation of individual skin layers confirmed that this non-linear skin behavior is largely dominated by the dermis, which is 2–3 times softer and thicker than the epidermis. Whereas the average secant shear modulus of the epidermis at a frequency of 1 Hz was ~6 kPa and of the epidermal/dermal papillary region ~3 kPa, the secant shear modulus of the (reticular) dermis was ~2 kPa, approximating the overall G_L=2.67 kPa.

Regarding the experimental procedure, skin samples were not hydrated during shear to make video recording for DIC possible. In order to detect potential dehydration artifacts, measurements were performed for minimal periods with short intervals between the measurements. In addition, the first shear condition was repeated after having performed measurements at all test conditions. Lissajous curves of these repeated measurements were compared and demonstrated that there was no significant stiffening effect of the samples (Fig. 8). Most likely skin was only marginally dehydrated due to short measuring periods after placing the sample from a liquid environment on the rheometer. Additionally, the dense character of skin as well as the physical skin properties most likely aided retention of water.

Skin is anisotropic and the orientation of skin relative to the Langer's lines (Langer, 1978) during mechanical testing has shown to be significant when tested in tensile/shear deformation (Annaidh et al., 2012; Liang et al., 2011). In the current study shear deformation of skin was measured in a random orientation. The results demonstrated that intra-patient variation increased with increasing strain amplitude (Fig. 3), indicating that orientation at small strain amplitudes may not have affected shear deformation, whereas at increasing strain amplitudes the effect of orientation may

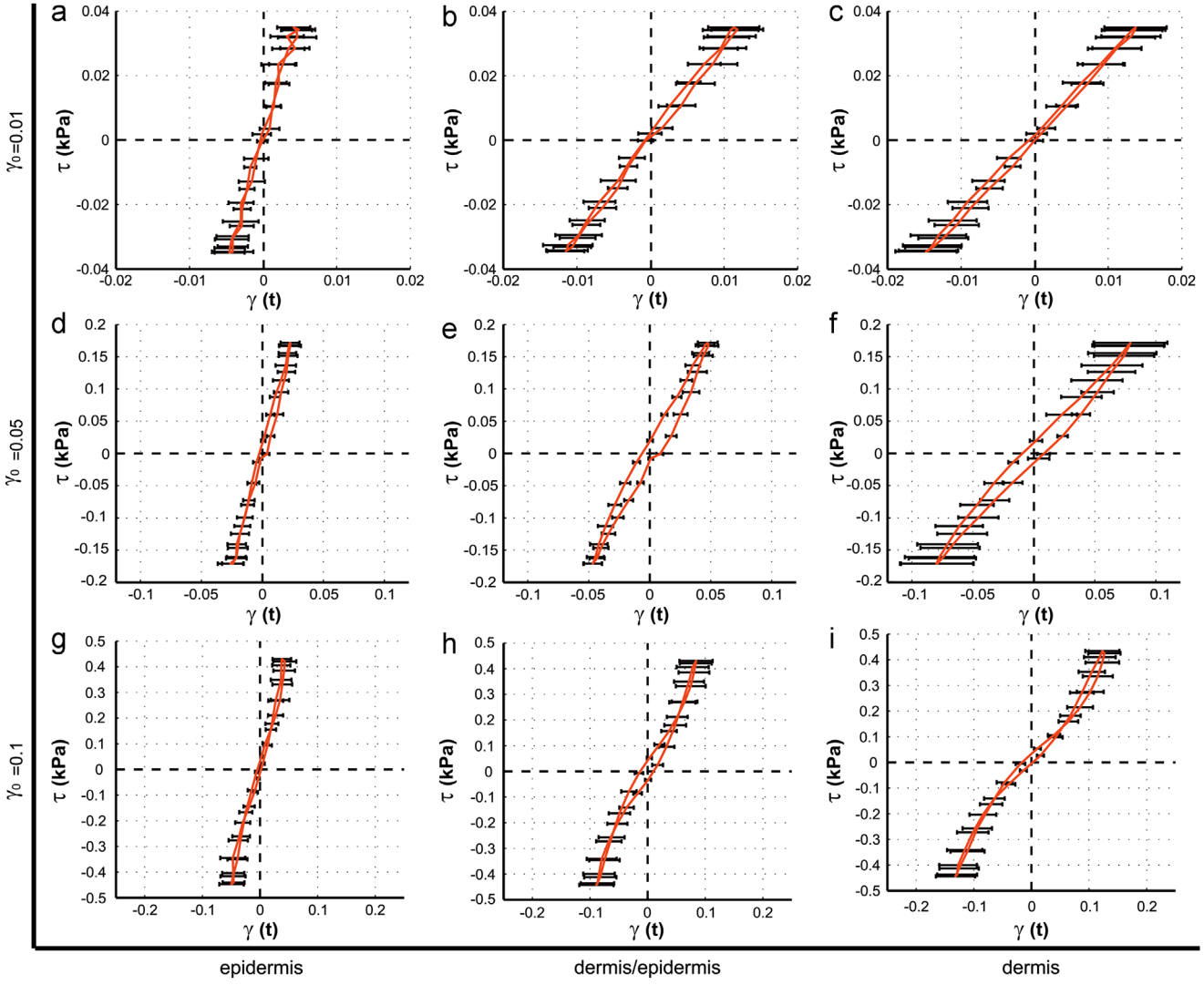

Fig. 6 – Decomposition of skin displacement into three different heights within skin at three strain amplitudes at a frequency of 1 Hz. ≥6 samples were tested per patient in 5 patients. Error bars represent 95% confidence limits.

have become more significant. On the other hand, the fibers in skin are only stretched slightly during shear deformation. Therefore, it is more probable that the large deviation in stiffness is a result of the heterogeneous composition of the skin samples, such as the structure of the epidermal papillae.

Shear moduli of through-plane skin found in the current study, corroborate results from suction and indentation analyses performed *in vivo* (Boyer et al., 2012; Jachowicz et al., 2007; Pailler-Mattei and Zahouani, 2004; Pailler-Mattei et al., 2007, 2008; Zahouani et al., 2011). Moduli derived from *in vitro* uniaxial tensile tests were up to three orders of magnitude higher (Annaidh et al., 2012; Jacquemoud et al., 2007). A major difference between tensile tests and shear experiments is that during uniaxial extension skin is homogeneously elongated over the three layers i.e. the layers are loaded in parallel and the stiffest layer will dominate, while in shear the layers are loaded in series and the softest one will dominate. In addition, fibers will be stretched and will play a much more dominant role in tension than in shear. Lastly, uniaxial tensile tests are usually performed at non-physiologically high strains (to the point of failure), by which a significant strain-stiffening effect is induced, resulting in increased Young's moduli. (Annaidh et al., 2012; Jacquemoud et al., 2007).

When decomposing skin into separate layers by DIC, our results are similar to those by Geerligs et al. (2011a), who reported that the epidermis had an average stiffness of 8 kPa and the dermis a stiffness of 2–3 kPa. However, the current study confirmed the hypothesis that mechanically, skin should not be considered as a three layered tissue, but as a continuously varying composite. DIC profiles of through-plane skin illustrated that shear moduli gradually decreased from 7–9 kPa at the outer epidermis layer down to 2 kPa at the dermis without forming a clear distinction between the layers or boundaries. This gradual decrease in stiffness can also be explained from a biological point of view. The cellular and fibrous composition of both the epidermis and dermis change with height (Venus et al., 2010). First, the epidermis is divided in several strata, which are biologically distinct. Whereas the epidermis and dermis are separated by the

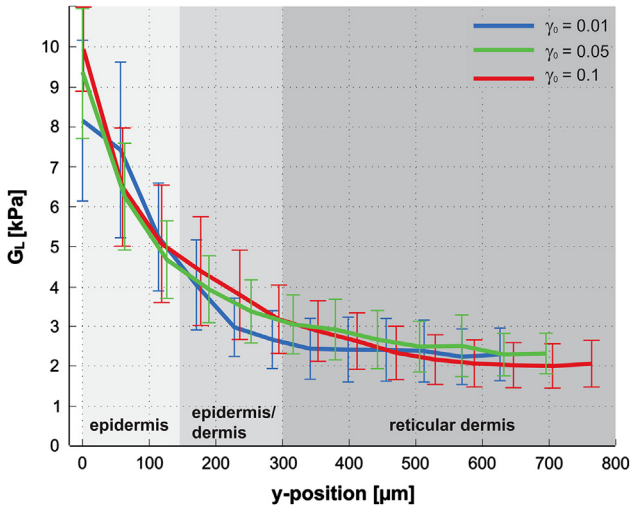

Fig. 7 – Secant shear moduli (G_L) profiles through full thickness skin samples at γ_0=0.01, 0.05, and 0.1 with a constant frequency of 1 Hz. ≥6 skin samples were tested per patient in 5 patients. Error bars represent 95% confidence limits.

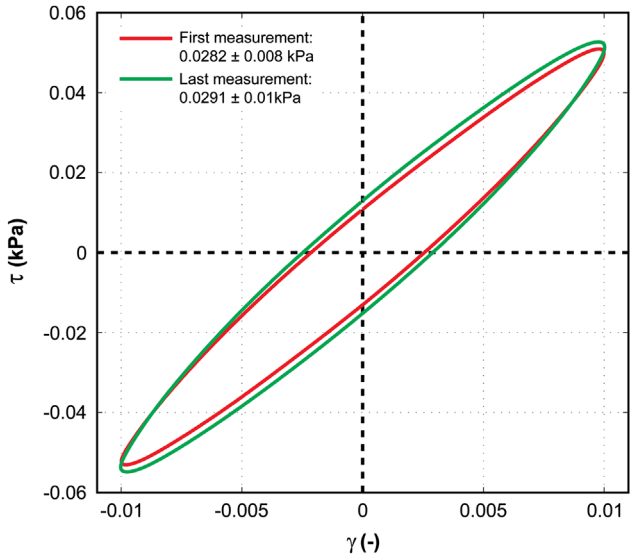

Fig. 8 – Dehydration effect of shear stress on skin in time at γ_0=0.01 with a frequency of 1 Hz.

dermal–epidermal junction, a papillary region consisting of epidermis and papillary dermis is still clearly observed. The underlying reticular dermis consists of fibers, which become more loosely distributed with increasing depth, resulting in a decreased shear modulus. In addition, the dermis contains many biological structures, such as hair follicles, sweat glands, and sebaceous glands. This may also have resulted in the heterogeneous deformation within skin, as observed in the skin deformation movies (Movies 1–3). However, since it was impossible to include such heterogeneities in the stress calculations, local displacements were averaged along the horizontal direction. To circumvent possible distortion in the results, shear experiments were performed on minimally six samples per patient and these results were averaged (Fig. 7).

It has been shown that the mechanical response of skin becomes non-linear upon increasing strains. Holt et al. (2008) demonstrated that full thickness skin displayed a strain stiffening effect upon shear deformations. In the current study, LAOS of full thickness skin proved to be complex with both intra-cycle strain stiffening and inter-cycle shear thinning (Fig. 2), which is common to soft materials (Ewoldt et al., 2008; Ma et al., 1999). Comparison of time revolved deformation between the epidermis and dermis (Fig. 6) confirmed that non-linear deformation within full skin was mainly resulting from the soft dermis and not from the stiff epidermis. Furthermore, during deformation at a γ_0=0.1 hysteresis became negative for the dermis at strains between 0.05 and 0.1 (Fig. 6h and i). In the thickness direction the properties vary. Any layer at an arbitrary height is not loaded by the prescribed boundary condition i.e. $\gamma_0 \sin(\omega t)$, however with a non-linear time-dependent shear stress that depends on the varying viscoelastic properties of skin between the plates and the layer under consideration. This may have led to negative hysteresis.

The complex behavior of particularly the dermis upon LAOS deformation may be explained by a three phase process. First, startup Lissajous curves confirmed that skin quickly changes to a steady deformation at large strain amplitudes. This short period of 2 s may be caused by a temporary structural change of large fiber reorganization in the dermis. Still, the fibers can retract to their native state, as observed during prolonged relaxation after LAOS up to γ_0=0.1. Secondly, subsequent shear thinning may be caused by the delayed (partial) retraction of the fibers after full extension, which is also shown by the decrease in G_M with increasing strain amplitudes (Fig. 5). Finally, upon increasing shear strain the fibers start to elongate again and experience tension, which is reflected by the observed strain stiffening effect. A similar effect of strain-induced stiffening has been reported for the viscoelastic proteins keratin and vimentin (Janmey et al., 1991; Ma et al., 1999). For confirmation of this hypothesis, LAOS experiments should be performed in combination with detailed imaging of elastic fiber deformation by for example confocal laser scanning microscopy.

In the current study, we obtained a full overview of the response of through-plane thickness human skin towards LAOS and three frequencies. The response of skin is affected by both strain amplitude and deformation frequency and is highly non-linear. Modeling skin behavior may aid the understanding of this complex behavior and also increase the predictability of skin deformation upon loading in practical situations. Furthermore, to obtain a full understanding of the biomechanical properties of human skin, it is important to correlate the shear response to the behavior in extension. Hereby, it is essential that not only through-plane skin samples are analyzed, but also separate skin layers, for obtaining a full understanding of the extension properties of human skin.

5. Conclusion

LAOS and DIC analyses from rheological measurements demonstrated that the mechanical response of skin becomes non-linear with increasing strain amplitudes. Moreover, it is shown that the epidermis has an average secant shear

modulus of 6 kPa and is ~3-fold stiffer than the relatively soft dermis. In conclusion, skin should be considered as a complex composite rather than a three layered tissue.

REFERENCES

Annaidh, A.N., Bruyere, K., Destrade, M., Gilchrist, M.D., Ottenio, M., 2012. Characterization of the anisotropic mechanical properties of excised human skin. Journal of the Mechanical Behavior of Biomedical Materials 5, 139–148.

Bhushan, B., Tang, W., 2011. Surface, tribological, and mechanical characterization of synthetic skins for tribological applications in cosmetic science. Journal of Applied Polymer Science 120, 2881–2890.

Boyer, G., Pailler-Mattei, C., Molimard, J., Pericoi, M., Laquieze, S., Zahouani, H., 2012. Non-contact method for in vivo assessment of skin mechanical properties for assessing effect of ageing. Medical Engineering and Physics 34, 172–178.

Cowley, K., Vanoosthuyze, K., 2012. Insights into shaving and its impact on skin. British Journal of Dermatology 166, 6–12.

Derler, S., Gerhardt, L.C., 2012. Tribology of skin: review and analysis of experimental results for the friction coefficient of human skin. Tribology Letters 45, 1–27.

Ewoldt, R.H., Hosoi, A.E., McKinley, G.H., 2008. New measures for characterizing nonlinear viscoelasticity in large amplitude oscillatory shear. Journal of Rheology 52, 1427–1458.

Geerligs, M., Oomens, C., Ackermans, P., Baaijens, F., Peters, G., 2011a. Linear shear response of the upper skin layers. Biorheology 48, 229–245.

Geerligs, M., van Breemen, L., Peters, G., Ackermans, P., Baaijens, F., Oomens, C., 2011b. In vitro indentation to determine the mechanical properties of epidermis. Journal of Biomechanics 44, 1176–1181.

Geers, M.G.D., DeBorst, R., Brekelmans, W.A.M., 1996. Computing strain fields from discrete displacement fields in 2D-solids. International Journal of Solids and Structures. 33, 4293–4307.

Gerhardt, L.C., Lenz, A., Spencer, N.D., Munzer, T., Derler, S., 2009. Skin-textile friction and skin elasticity in young and aged persons. Skin Research and Technology 15, 288–298.

Gerhardt, L.C., Schmidt, J., Sanz-Herrera, J.A., Baaijens, F.P.T., Ansari, T., Peters, G.W.M., Oomens, C.W.J., 2012. A novel method for visualising and quantifying through-plane skin layer deformations. Journal of the Mechanical Behavior of Biomedical Materials 14, 199–207.

Girardeau, S., Mine, S., Pageon, H., Asselineau, D., 2009. The Caucasian and African skin types differ morphologically and functionally in their dermal component. Experimental Dermatology 18, 704–711.

Hendriks, F.M., Brokken, D., Oomens, C.W.J., Baaijens, F.P.T., 2004. Influence of hydration and experimental length scale on the mechanical response of human skin in vivo, using optical coherence tomography. Skin Research and Technology 10, 231–241.

Holt, B., Tripathi, A., Morgan, J., 2008. Viscoelastic response of human skin to low magnitude physiologically relevant shear. Journal of Biomechanics 41, 2689–2695.

Hyun, K., Wilhelm, M., Klein, C.O., Cho, K.S., Nam, J.G., Ahn, K.H., Lee, S.J., Ewoldt, R.H., McKinley, G.H., 2011. A review of nonlinear oscillatory shear tests: analysis and application of large amplitude oscillatory shear (LAOS). Progress in Polymer Science 36, 1697–1753.

Jachowicz, J., McMullen, R., Prettypaul, D., 2007. Indentometric analysis of in vivo skin and comparison with artificial skin models. Skin Research and Technology 13, 299–309.

Jacquemoud, C., Bruyere-Garnier, K., Coret, M., 2007. Methodology to determine failure characteristics of planar soft tissues using a dynamic tensile test. Journal of Biomechanics 40, 468–475.

Janmey, P.A., Euteneuer, U., Traub, P., Schliwa, M., 1991. Viscoelastic properties of vimentin compared with other filamentous biopolymer networks. Journal of Cell Biology 113, 155–160.

Krueger, N., Luebberding, S., Oltmer, M., Streker, M., Kerscher, M., 2011. Age-related changes in skin mechanical properties: a quantitative evaluation of 120 female subjects. Skin Research and Technology 17, 141–148.

Langer, K., 1978. Anatomy and physiology of skin.1. Cleavability of cutis. British Journal of Plastic Surgery 31, 3–8.

Liang, X., Boppart, S.A., 2010. Biomechanical properties of in vivo human skin from dynamic optical coherence elastography. IEEE Transactions on Biomedical Engineering 57, 953–959.

Liang, X., Graf, B.W., Boppart, S.A., 2011. In vivo multiphoton microscopy for investigating biomechanical properties of human skin. Cellular and Molecular Bioengineering 4, 231–238.

Ma, L.L., Xu, J.Y., Coulombe, P.A., Wirtz, D., 1999. Keratin filament suspensions show unique micromechanical properties. Journal of Biological Chemistry 274, 19145–19151.

MacNeil, S., 2008. Biomaterials for tissue engineering of skin. Materials Today 11, 26–35.

Meyers, M.A., Chen, P.Y., Lin, A.Y.M., Seki, Y., 2008. Biological materials: structure and mechanical properties. Progress in Materials Science 53, 1–206.

Minematsu, T., Yamamoto, Y., Nagase, T., Naito, A., Takehara, K., Iizaka, S., Komagata, K., Huang, L.J., Nakagami, G., Akase, T., Oe, M., Yoshimura, K., Ishizuka, T., Sugama, J., Sanada, H., 2011. Aging enhances maceration-induced ultrastructural alteration of the epidermis and impairment of skin barrier function. Journal of Dermatological Science 62, 160–168.

Nicolle, S., Palierne, J.-F., 2012. On the efficiency of attachment methods of biological soft tissues in shear experiments. Journal of the Mechanical Behavior of Biomedical Materials 14, 158–162.

Oomens, C.W.J., Vancampen, D.H., Grootenboer, H.J., 1987. A mixture approach to the mechanics of skin. Journal of Biomechanics 20, 877–885.

Pailler-Mattei, C., Bec, S., Zahouani, H., 2008. In vivo measurements of the elastic mechanical properties of human skin by indentation tests. Medical Engineering and Physics 30, 599–606.

Pailler-Mattei, C., Pavan, S., Vargiolu, R., Pirot, F., Falson, F., Zahouani, H., 2007. Contribution of stratum corneum in determining bio-tribological properties of the human skin. Wear 263, 1038–1043.

Pailler-Mattei, C., Zahouani, H., 2004. Study of adhesion forces and mechanical properties of human skin in vivo. Journal of Adhesion Science and Technology 18, 1739–1758.

Pan, B., Qian, K.M., Xie, H.M., Asundi, A., 2009. Two-dimensional digital image correlation for in-plane displacement and strain measurement: a review. Measurement Science and Technology 20 Art.no. 062001.

Tang, W., Bhushan, B., Ge, S., 2010. Friction, adhesion and durability and influence of humidity on adhesion and surface charging of skin and various skin creams using atomic force microscopy. Journal of Microscopy 239, 99–116.

Venus, M., Waterman, J., McNab, I., 2010. Basic physiology of the skin. Surgery 28, 469–472.

Wilhelm, M., 2002. Fourier-transform rheology. Macromolecular Materials and Engineering 287, 83–105.

Zahouani, H., Boyer, G., Pailler-Mattei, C., Ben Tkaya, M., Vargiolu, R., 2011. Effect of human ageing on skin rheology and tribology. Wear 271, 2364–2369.